HHS Public Access

Author manuscript

Biomacromolecules. Author manuscript; available in PMC 2022 November 22.

Published in final edited form as:

Biomacromolecules. 2021 August 09; 22(8): 3613–3623. doi:10.1021/acs.biomac.1c00712.

Isolation of Cowpea Mosaic Virus-Binding Peptides

Soo Khim Chan,

Department of NanoEngineering, University of California, San Diego, La Jolla, California 92039, United States

Nicole F. Steinmetz

Department of NanoEngineering, Department of Bioengineering, Department of Radiology, Center for Nano-ImmunoEngineering, Moores Cancer Center, and Institute for Materials Discovery and Design, University of California, San Diego, La Jolla, California 92039, United States

Abstract

The plant virus cowpea mosaic virus (CPMV) is a natural nanocarrier that has been developed as a platform technology for the delivery of various payloads including peptide epitopes for vaccines, contrast agents for imaging, and drugs for therapy. Genetic fusion and chemical conjugations are the mainstay approaches to load the active ingredient to the exterior and/or interior of CPMV. However, these methods have limitations; genetic engineering is limited to biologics, and chemical alteration often requires multistep reactions with modification of both CPMV and the active ingredient. Either method can also result in particle instability. Therefore, to provide an alternate path toward CPMV functionalization, we report the isolation of peptides that specifically bind to CPMV, termed CPMV-binding peptides (CBP). We used a commercial M13 phage display 7-mer peptide library to pan for and select peptides that selectively bind to CPMV. Biopanning and characterization of lead candidates resulted in isolation of the motif “GWRVSEF/L” as the CPMV-specific motif with phenylalanine (F) at the seventh position being stronger than leucine (L). Specificity to CPMV was demonstrated, and cross-reactivity toward other plant viruses was not observed. To demonstrate cargo loading, GWRVSEF was tagged with biotin, fluorescein isothiocyanate (FITC), and a human epidermal growth factor receptor 2 (HER2)-specific targeting peptide ligand. Display of the active ingredient was confirmed, and utility of tagged and targeted CPMV in cell binding assays was demonstrated. The CBP functionalization strategy offers a new avenue for CPMV nanoparticle functionalization and should offer a versatile tool to add active ingredients that otherwise may be difficult to conjugate or display.

Corresponding Author: Nicole F. Steinmetz – nsteinmetz@ucsd.edu.

Author Contributions

S.K.C. designed and performed the experimental work. N.F.S. conceived the study and oversaw the design and testing. S.K.C. and N.F.S. wrote the manuscript. All authors read and edited the manuscript.

The authors declare the following competing financial interest(s): Dr. Steinmetz is a co-founder of and has a financial interest with Mosaic ImmunoEngineering Inc. Dr. Chan declares no competing financial interests.

Complete contact information is available at: https://pubs.acs.org/10.1021/acs.biomac.1c00712

Supporting Information

The Supporting Information is available free of charge at https://pubs.acs.org/doi/10.1021/acs.biomac.1c00712.

Figures S1–S3 and Tables S1 and S2, showing plant viruses/virus-like particle characterization, enrichment factor, and calculation of number peptide per CPMV (PDF)

Graphical Abstract

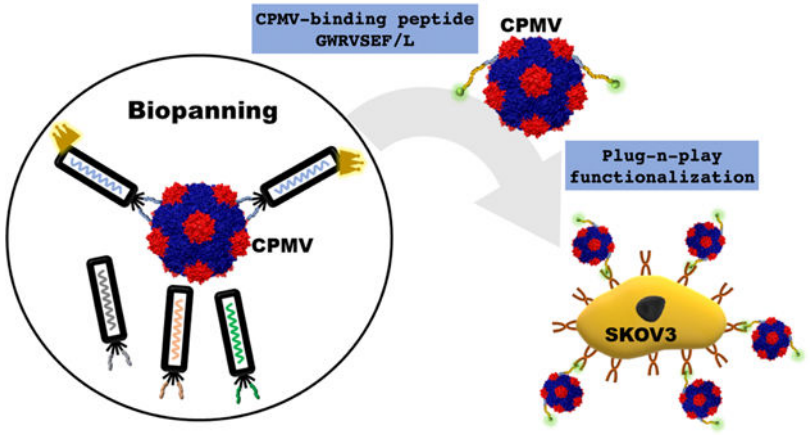

INTRODUCTION

Cowpea mosaic virus (CPMV) is a member of the family *Secoviridae*. The bipartite positive sense RNA plant virus forms ~30 nm sized pseudo-T3 icosahedral proteinaceous capsids composed of 60 copies each of a large (L, 42 kDa) and a small (S, 24 kDa) coat protein.[1,2] Ever since the discovery of CPMV in West Africa in the late 1950s,[3] this nanoscale scaffold has been studied extensively and made impactful progress in many aspects of nanomedicine research. CPMV-based nanotechnology has been applied as a vaccine platform, immunotherapy, imaging applications, and drug delivery.[4,5] Aside from acting as an adjuvant for vaccines and immunotherapy,[6,7] CPMV capsids can be engineered to carry active ingredients such as peptides,[8] therapeutics,[9] fluorophores,[10] and contrast agents.[9] In fact, CPMV was one of the first plant viruses developed as peptide display system[11,12] because of its biocompatibility and high degree of thermal and structural stability.[9]

Active ingredients can be loaded and conjugated to the exterior or interior surface via covalent coupling to the coat proteins; cargo can also be infused into the nanoparticle by making use of the porous nature of the viral capsid and the chemically distinct interior/exterior environments.[10,13,14] A variety of chemical bioconjugation tools are available to modify CPMV, that is, targeting solvent-exposed lysine side chains by using the *N*-hydroxysuccinimidyl ester (NHS) reaction and biorthogonal click chemistry such as copper-catalyzed azide–alkyne cycloaddition (CuAAC).[15] The interior can be selectively modified, targeting cysteine side chains on the interior capsid surface,[16] with nucleic acid-free virus-like particles of CPMV being more reactive toward this coupling strategy.[17] As an alternative, genetic fusion of biological cargo can be achieved by targeting surface loops;[11,18] the βB–βC loop on the small coat protein is most commonly used for insertion because it is highly accessible.[19] While highly versatile, each approach has its limitations: genetic engineering is limited to biologics with a peptide length <40 amino acids and isoelectric point <9.0,[18] and chemical modification often requires multistep reactions requiring modification of both the CPMV carriers and its target active ingredient. Either method can pose the risk of destabilizing the viral protein structure.[13]

As a new direction, we set out to develop a noncovalent yet CPMV-specific modification strategy; specifically, we isolated CPMV binding peptides via phage display technology.[20] Here, peptides against CPMV are isolated through repetitive cycles of affinity selections (i.e., biopanning). The direct linkage between the genotype (gene encoding the displayed moiety) and phenotype (displayed moiety) allows the bound moieties that displayed on phage to be identified via DNA sequencing.[21] Here we used a commercial M13 phage display 7-mer peptide library to pan for and select peptides binding to CPMV. The isolated CPMV-binding peptides (termed CBP) were validated and selectivity, specificity, and affinity determined by using a combination of Western blot, native agarose gel electrophoresis, enzyme-linked immunosorbent assay (ELISA), and immunogold staining followed by transmission electron microscopy (TEM). Toward applications, we also demonstrated that CPMV can be functionalized using dual-functional peptides containing the CBP domain and a receptor-targeting domain; here human epidermal growth factor receptor 2 (HER2) was targeted by using a peptide ligand. Cancer cell vs immune cell uptake of the CBP-functionalized CPMV carrying the HER2 ligand was monitored by using flow cytometry to assay for targeted vs nonspecific cell uptake.

MATERIALS AND METHODS

Cowpea Mosaic Virus (CPMV) Preparation and Characterizations.

Cowpea mosaic virus (CPMV) was produced in *Vigna unguiculata* plants by infecting each primary leave with 4 μg of CPMV via mechanical inoculation (4 μg of CPMV was added per leaf in 40 μL of 0.1 M potassium phosphate buffer (pH 7.0) after leaves were dusted with carborundum). Infected leaves were harvested 12 days postinfection and purified as previously described.[22] The concentration of purified CPMV was determined by ultraviolet–visible (UV–vis) at wavelength 260 nm with the extinction coefficient ε(260 nm) = 8.1 $(\text{mg/mL})^{-1}$ cm^{-1}. CPMV preparations were characterized by transmission electron microscopy (TEM), dynamic light scattering (DLS), agarose gel electrophoresis, and size exclusion chromatography (SEC), as previously reported.[23]

Isolation of CPMV-Binding Peptides by Biopanning.

The Ph.D.-7 Phage Display Peptide Library Kit (New England Biolabs) with 10^9 unique sequences was used for isolation of CPMV binding peptides. 5 μg of CPMV was coated into each well of Nunc Maxisorp flat-bottom 96-well plates and incubated overnight at 4 °C. 10^9 pfu of the pre-blocked phage library (in 2% (w/v) bovine serum albumin; BSA) was added after the following blocking steps to remove BSA binders. The next day, CPMV was drained off and the well blocked with 2% (w/v) BSA for 1 h at room temperature (rt) with shaking at 800 rpm. The wells were washed thrice with Tris-buffered saline with 0.1% (v/v) Tween-20 (TBST) for 1 min per wash. The phage library was then added into the well and incubated for 30 min at rt with shaking at 800 rpm. The wells were washed thrice with TBST for 5 min per wash to remove unbound phages. The concentration of Tween-20 in TBST was increased from 0.1% to 0.3% and then 0.5% for each subsequent round to increase the selection stringency. Bound phages were eluted from CPMV by incubation with 0.2 M glycine–HCl (pH 2.2) for 18 min at rt and immediately neutralized by adding 1

M Tris–HCl buffer (pH 9.1). The eluted phages were subjected for amplification and titer according to the manufacturer's protocol.

Monoclonal Enzyme-Linked Immunosorbent Assay (ELISA).

5 μg of CPMV (in 0.1 M bicarbonate buffer, pH 8.6) was coated into each well of a Nunc Maxisorp flat-bottom 96-well plate and incubated overnight at 4 °C. 2% (w/v) BSA was also coated to serve as negative control. The next day, the plate was blocked with 2% (w/v) BSA and incubated at rt with shaking at 800 rpm for 1 h. Subsequently, the plate was washed thrice with 0.1% TBST for 1 min. 100 μL of amplified phage from the last biopanning cycle was added into each well followed by incubation at rt with shaking at 800 rpm for 1 h. Later, the plate was washed thrice with 0.5% TBST for 5 min. 100 μL of 1:500 dilution of HRP-conjugated anti-M13 monoclonal antibody (Abcam ab50370) was added and incubated at rt for 1 h with shaking at 800 rpm. The plate was again washed thrice with 0.5% TBST for 5 min followed by adding 100 μL of tetramethylbenzidine (TMB) substrate (Thermo Scientific Pierce) into each well. The plate was incubated in the dark for 10 min, and the absorbance was measured at 370 nm by using an Infinite 200 Rx plate reader (Tecan Life Sciences) with 25 flashes in 96-well flat-bottom plate mode. Monoclonal phages with at least 0.3 difference in absorbance value between CPMV and BSA were subjected for DNA sequencing (Eurofins Genomics).

Validation of Monoclonal Phage.

Binding of monoclonal phages to CPMV was validated by three separate assays:

Dot Blot.—10^9 pfu of phage was coated on Amersham Protran 0.45 nitrocellulose membrane (GE Healthcare) and air-dried in a hood for 10 min. The membrane was blocked with 2% (w/v) BSA for 1 h at rt followed by three washing steps with 0.1% TBST for 1 min. 100 μg of CPMV in 0.1% TBST was added to the membrane followed by incubation at rt for 30 min with shaking at 800 rpm. Membranes were then washed thrice with 0.5% TBST for 5 min. Polyclonal anti-CPMV antibodies (1:500 dilution; custom-made through immunization of rabbits) in 2% (w/v) BSA was added to the membranes and incubated for 1 h with shaking at 800 rpm. Membranes were washed again with 0.5% TBST thrice prior to adding HRP-conjugated goat anti-rabbit antibodies (1:5000 dilution; Pacific Immunology) in 2% (w/v) BSA and incubated for 1 h at rt with shaking at 800 rpm. The membrane was then washed with 0.5% TBST prior to incubation with 1 mL of Pierce ECL Western blotting substrate for 1 min. Lastly, membrane was exposed to the chemiluminescence mode for 40 s with ProteinSimple FluorChem R.

Cross-Reactivity Assay.—5 μg of virus particles was coated in Nunc Maxisorp flat-bottom 96-well plate, and ELISA assays were performed similarly to the "Monoclonal ELISA" with one modification: 10^9 pfu of phage was added into each well to test their binding to the coated virus particles.

Titration ELISA.—Two-fold serial dilutions of CPMV (40, 20, 10, 5, 2.5, 1.25, 0.63, 0.31, 0.16, 0.08, and 0 μg) were coated in a Nunc Maxisorp flat-bottom 96-well plate, and ELISA

was performed similarly to the “monoclonal ELISA” with one modification: 10^9 pfu of phage was added into each well for binding.

Peptide Conjugation and Characterizations.

CPMV-Binding Peptides (CBP).—CBP-biotin (N-GWRVSEFGGGSK/biotin/-C) and CBP-FITC (N-GWRVSEFGGGSK/FITC/-C) were synthesized by GenScript with 75% purity. Binding of CBP-biotin or CBP-FITC peptide to CPMV was performed by incubating a 500-fold molar excess of peptide per CPMV; the mixture was allowed to react overnight at 4 °C. Complexed product, i.e., CPMV-CBP-biotin and CPMV-CBP-FITC, was purified by using PD MiniTrap desalting columns with Sephadex G-25 resin (Cytiva) followed by 100 kDa Amicon Ultra-0.5 centrifugal unit (dual-step purification). The concentration of the final product was determined by Nanodrop as described above. Particle integrity was validated by DLS and TEM as described above.

HER2 Targeting Ligands: CBP-AHNP Peptides.—CBP-AHNP (N-GWRVSEF-KKKKKKKKDDDD-FCDGFYACYMDVK/FITC/-C) and *AHNP (N-KKKKKKKKDDDD-FCDGFYACYMDVK/FITC/-C) were synthesized by GenScript with 75% purity. Binding of CBP-AHNP and *AHNP control peptide (the latter lack the CBP domain) to CPMV was performed by incubating a 100-fold molar excess peptide per CPMV and incubation at 37 °C for 1 h. Purification and quantification of the product were determined to be described above.

Validation of CBP Binding to CPMV.

Binding of CPMV–peptide to CPMV was determined by five different approaches as follows:

Agarose Gel Electrophoresis.—10 μg of CBP-FITC peptide conjugated CPMV was loaded onto a 1.2% (w/v) TAE agarose gel. 10 μg of CPMV and 0.1 μg of free CBP-FITC peptide were loaded as control. The samples were electrophoresed at 110 V for 40 min.

Peptide ELISA. For CPMV-CBP-FITC.—Serial dilutions of CPMV (10, 5, 2.5, 0.125, 0.63, 0.31, 0.16, 0.08, 0.04, and 0.02 μg) were coated in a Corning 96-well solid white flat-bottom polystyrene microplate. The plate was incubated overnight at 4 °C followed by blocking with 2% (w/v) BSA at rt for 1 h with shaking at 800 rpm. The plate was then washed thrice with 0.1% TBST, and 0.1 μg of CBP-FITC peptide was added into each well. After incubation for 30 min at rt with shaking at 800 rpm, the plate was washed thrice with 0.5% TBST for 5 min. 100 μL of distilled water was added into each well, and fluorescent reading was taken with an Infinite 200 Rx plate reader (Tecan Life Sciences) with excitation and emission at 495 and 519 nm.

For CPMV-CBP-Biotin.—1 μg of CBP-biotin peptide was coated in Pierce streptavidin-coated immunoassay plates, 96-well (Thermo Scientific), and incubated 1 h at rt with shaking at 800 rpm. The plate was blocked with 2% (w/v) BSA followed by three washings with 0.1% TBST for 1 min per wash. 5 μg of CPMV was added for binding and incubated for 1 h at rt with shaking at 800 rpm. Then the plate was washed thrice with 0.5% TBST for

5 min each wash. 100 μL of anti-CPMV rabbit polyclonal antibodies (1:500 dilution) was added to the wells followed by incubation at rt for 1 h with shaking at 800 rpm. Following three washing steps using 0.5% TBST for 5 min, 100 μL of HRP conjugated goat anti-rabbit antibodies (1:5000 dilution; Pacific Immunology) was added to the wells and incubated at rt for 1 h with shaking at 800 rpm. Finally, the plate was washed thrice with 0.5% TBST followed by adding 100 μL of TMB substrate (Thermo Scientific Pierce) into each well. The plate was incubated in the dark for 5–10 min, and the reaction was stopped with 50 μL of 2 N H_2SO_4. The absorbance was measured at 450 nm by using an Infinite 200 Rx plate reader (Tecan Life Sciences) with 25 flashes in 96-well flat-bottom plate mode.

Competitive ELISA.—Competitive ELISA was performed as mentioned in the "Monoclonal ELISA" with modifications. Two-fold serial dilutions of the CBP (0.500, 0.250, 0.125, 0.063, 0.031, 0.016, 0.008, 0.004, and 0.002 μg) were added separately into the well together with 10^9 pfu of monoclonal phages. The reaction after incubation with TMB substrate was stopped with 50 μL of 2 N H_2SO_4. Colorimetric detection was performed by measurement at 450 nm using an Infinite 200 Rx plate reader (Tecan Life Sciences) with 25 flashes in 96-well flat-bottom plate mode.

Western Blot.—10 μg of CPMV was loaded onto a NuPage 12% bis-tris gel (Thermo Fisher Scientific) and electrophoresed for 40 min at 200 V. Proteins were then blotted onto Amersham Protran 0.45 nitrocellulose membrane (GE Healthcare) at 25 V for 2 h. The membrane was then blocked with 5% (w/v) BSA for 1 h at rt with gentle shaking. Subsequently, the membrane was washed thrice with 0.5% TBST for 1 min. 1 μg/mL of CBP-biotin was added to the membrane for 1 h incubation at rt. The membrane was then washed with 0.5% TBST for 5 min. 100 μL of 1:500 dilution of HRP-conjugated Streptavidin-HRP conjugate (Abcam ab7403) was added and incubated at rt for 1 h. Following three washes with 0.5% TBST, the membrane was developed with a DAB substrate kit, peroxidase HRP (Vector Laboratories), for 5–10 min. The DAB reagent was drained off, and the bands were documented with ProteinSimple FluorChem R.

TEM Immunogold Binding.—20 μL of CPMV-CBP-biotin was place on Formvar/carbon-coated 400 mesh copper grids (Electron Microscopy Science) for 20 min. The grid was washed once with 10 mM KP buffer, pH 7, and blocked with 1% (w/v) BSA in 0.1% (v/v) Tween-20 for 30 min followed by equilibration in 0.1% (w/v) BSA in 0.1% (v/v) Tween-20 for 5 min. Later, the grid was then placed onto 20 μL of streptavidin-conjugated gold nanoparticles (5 nm sized gold, Nanocs) and incubated for 2 h. Following the incubation, the grid was washed four times with 0.01% TBST (3 min each wash), twice with 10 mM KP buffer (3 min each wash), and thrice with distilled water (5 min each wash). Lastly, the grid was stained with 2% (w/v) uranyl acetate (Fisher Scientific) for 2 min. Excess solution was blotted with filter paper. The grid was imaged with a FEI Tecnai G2 Spirit transmission microscope at 80 kV.

Flow Cytometry Analysis.

RAW 264.7 macrophages and SKOV3 cells were used for cell uptake assays. First, RAW 264.7 cells (200000 cells per well using V-bottom-shaped 96-well plates) were incubated

with 10 μg of CPMV for CPMV-CBP complexes for 1 h at 37 °C. The cells were then washed twice with FACS buffer (1 mM EDTA, 25 mM HEPES, 1% (v/v) FBS and topped up with 1 × PBS) and fixed with 2% (v/v) paraformaldehyde at rt for 15 min. The cells were then washed thrice with FACS buffer followed by permeabilization using FACS buffer with 0.5% (v/v) saponin. Next, cells were incubated with anti-CPMV rabbit polyclonal antibodies (1:500 dilution in FACS buffer) at 4 °C for 1 h; this was followed by two washes with FACS buffer with 0.5% (v/v) saponin. Secondary antibody (Cy5-conjugated goat anti-rabbit IgG antibody, Invitrogen) in FACS buffer with 0.5% (v/v) saponin and 5% (v/v) goat serum was then added to cells and incubated at 4 °C for 1 h. Finally, cells were washed twice with FACS buffer and resuspended in FACS buffer prior performing flow cytometry analysis using a BD Accuri C6 Plus flow cytometer.

For SKOV3 cell binding studies, cells were at 4 °C throughout the assay. Cells were first washed with cold FACS buffer with 0.1 (w/v) sodium azide (FACS-SA) followed by incubation with CPMV for CPMV-CBP complexes as described above. The cells were washed twice with FACS-SA buffer and fixed and stained as above (by omitting the permeabilization steps). Cells were analyzed by using a BD Accuri C6 Plus flow cytometer.

RESULTS AND DISCUSSION

Production and Characterization of CPMV.

CPMV was propagated and purified from black-eyed peas and used for isolation of CPB. Purified CPMV was characterized by sodium dodecyl sulfate polyacrylamide gel electrophoresis (SDS-PAGE), native agarose gel electrophoresis, transmission electron microscope (TEM), dynamic light scattering (DLS), and size exclusion chromatography (SEC), as shown in Figure 1. CPMV showed two distinct bands on denaturing SDS-PAGE (Figure 1A) characteristic for the L (42 kDa; black triangle) and S (24 kDa; open triangle) proteins; protein contaminants were not detectable. The colocalization of nucleic acids and the CPMV capsids (protein) on native agarose gel (Figure 1B) indicates that CPMV preparation yielded intact particles encapsidating their RNA molecules. TEM (Figure 1C) and DLS (Figure 1D) confirmed the presence of monodisperse CPMV with a hydrodynamic diameter of 32 nm and low polydispersity index (PDI ~ 0.06). SEC profiles further corroborated the presence of intact CPMV particles; aggregates or broken particles were not observed, and coelution of nucleic acid (260 nm) and protein (280 nm) from the Superose6 column was evident (Figure 1E).

Isolation and Validation of CPMV-Binding Monoclonal Phage.

A commercial Ph.D.-7 Phage Display Peptide Library Kit (NEB) was used to isolate potential peptide binders against CPMV. The 7-mer peptide library consisted of 10^{13} pfu/mL M13 phage displayed particles with 10^{9} unique peptides fused to the amino terminus of the minor coat protein pIII of M13 phage.[24] The input library was preincubated overnight with blocking agent (2% (w/v) bovine serum albumin; BSA) each round to remove potential BSA binders. Three rounds of selections (biopanning) were performed to enrich CPMV binders by increasing the washing stringency (Tween-20 concentration was increased from 0.1% to 0.3% to 0.5% (v/v)) to remove nonspecific and/or weak binders. Approximately 33-fold

enrichment was observed from three rounds of biopanning (Table S1). Forty monoclonal phages were randomly selected from the enriched phage pool to perform monoclonal enzyme-linked immunosorbent assay (ELISA) against CPMV and BSA (negative control) (Figure 2A). Monoclonal phages yielding an absorbance difference of 0.2 units comparing CPMV vs BSA binding were selected for DNA sequencing.

Twenty-seven clones were in-frame with the plasmid backbone (two clones were either empty or out-of-frame) and sequencing yielded four unique sequence categories (Figure 2B). 89% of the in-frame clones displayed the motif GWRVSEF, and 3.7% displayed highly identical motif “GWRVSEL” suggesting the consensus sequence “GWRVSE” as the CPMV binding motif. The third unique peptide sequence “GFHYSLH” also showed a certain degree of homology with motif “GXXXSXX”. The fourth identified peptide sequence “IVGSQVT” contains several identical amino acids (V, G, S) found in “GWRVSEF” but at different positions. Because peptide “IVGSQVT” had low similarity to the other candidate sequences, it was excluded from further study. We note that lack of homology does not reflect that peptide IVGSQVT is not a true CPMV binder. Nevertheless, MPSEF was highly enriched, covering almost 90% of the monoclonal phages binding to CPMV; therefore, in this work we decided to investigate the homologous sequences only. Hereafter, monoclonal phages with peptide sequence GWRVSEF, GWRVSEL, and GFHYSLH were designated as MP_{SEF}, MP_{SEL}, and MP_{SLH}, respectively.

Cross-reactivity of monoclonal phages (MP_{SEF}, MP_{SEL}, and MP_{SLH}) was tested comparing their binding to CPMV versus other nonrelated plant viruses, specifically tobacco mosaic virus (TMV) and tobacco mild green mosaic virus (TMGMV), both of which are 300 × 18 nm tubular plant viruses; potato virus X (PVX) a 515 × 13 filamentous plant virus; and physalis mottle virus (PhMV) and cowpea chlorotic mottle virus (CCMV); both form —like CPMV—30 nm sized icosahedrons. It should be noted that PhMV was expressed in *E. coli* and used as a virus-like particle (VLP); all other plant viruses were produced in plants as plant viruses containing their genome. The methods for virus production and characterization (SDS-PAGE and TEM) are detailed in the Supporting Information and Figure S1. Binding assays revealed high binding of MP_{SEF} and MP_{SEL} to CPMV with MP_{SEF} exhibiting stronger binding as indicated by higher absorbance intensity read-out (Figure 2C). Importantly, MP_{SEF} and MP_{SEL} phages demonstrated specificity toward CPMV with negligible or no interactions with any other viruses tested. MP_{SLH}, on the contrary, showed no binding to any of the plant viruses tested—not even to CPMV or the empty M13 phage (M13KE). Enrichment of this nonspecific false-positive binder might be due to its binding to one of the components used in the biopanning process and/or failure to be removed during the washing step. Presence of nontarget binders in enriched pool of phages is a common observation, and hence downstream verification is critical.[25] We concluded that the motif “GWRVSEF/L” is the CPMV-specific motif with phenylalanine (F) at the seventh position being stronger than leucine (L). The three monoclonal phages (MP_{SEF}, MP_{SEL}, and MP_{SLH}) were then used for titration ELISA across a range of CPMV concentration (Figure 2D). The result is in congruent with Figure 2C where both the MP_{SEF}, and MP_{SEL} bound to CPMV, with MP_{SEF} showing higher binding affinity. MP_{SLH} showed no binding to CPMV.

Lastly, binding of MP_{SEF}, which showed the highest affinity for CPMV, was further assessed by using a dot blot. In this approach the polystyrene surface is replaced with a nitrocellulose membrane, and therefore this allowed to rule out the possibility of false positive binding due to adsorption to polystyrene. This is important because several studies have reported polystyrene binders within phage clones (also known as plastic binders). These target unrelated peptides (TUPs) are usually rich in hydrophobic amino acids to interact with the benzene ring of polystyrene.[26,27] Enrichment of these TUPs would lead to isolation of false positive clones. However, Figure 2E confirms the isolated peptide is not a TUP because MP_{SEF} bound to CPMV using the dot blot technique and in the absence of polystyrene.

Assessment of Synthetic CPMV-Binding Peptide (CBP) Binding to CPMV.

The peptide sequence GWRVSEF from the MP_{SEF} phage (termed CPMV-binding peptide, or, CBP) was synthesized with two separate modifications at the C-terminus (C-terminal modifications were chosen because the N-terminus is exposed and free when displayed on the M13 phage): CBP-biotin and CBP-fluorescein isothiocyanate (CBP-FITC) were synthesized to assay the interactions of the synthetic CBP peptides with CPMV. First, CBP-FITC or CBP-biotin binding to CPMV was tested by incubating the peptide at 500 molar excess in 0.1 M potassium phosphate (KP) buffer (pH 7) overnight at 4 °C. This was followed by sequential purification by using Sephadex desalting columns (G-25 resin) and 100 kDa molecular weight cutoff centrifugal filter membrane to remove excess peptides from the resulting CPMV-CBP-FITC complex or CPMV-CBP-biotin complex. The dual-step purification was found to be efficient in removing free CBP-FITC: free CBP-FITC could not be detected after purification (Figures S2 and S3). CPMV-CBP-FITC and CPMV-CBP-biotin remained stable and intact upon complexation with either peptide (CBP-FITC or CBP- biotin) as confirmed by DLS and TEM micrographs (Figure 3A). The fluorescent construct CPMV-CBP-FITC was analyzed by native agarose gel electrophoresis. Imaging under UV light followed by nucleic acid and protein staining indicates colocalization of the FITC label (chemiluminescence panel, Lane 2), nucleic acids (GelRed stain panel, Lane 2), and protein (Coomassie blue panel, Lane 2; Figure 3B). Binding of CBP-FITC to CPMV did not alter its electrophoretic mobility. By use of UV/vis spectroscopy and the CPMV and FITC-specific extinction coefficient, it was estimated that ~6 CBP-FITC peptides were per each CPMV particle (Table S2).

To assay the CPMV-CBP-biotin complex, a modified Western blot and TEM immunogold staining were used. For the modified Western blot, CPMV was denatured, and the coat proteins were separated by SDS-PAGE and transferred onto a nitrocellulose membrane. The coat proteins were then exposed to CBP-biotin followed by staining the biotin labels by using a streptavidin–HRP conjugate. Data confirmed that CBP-biotin peptides were indeed bound to the CPMV coat proteins, and binding was observed to the S and L protein (Figure 3C). Together, data indicate that CBP recognize the native CPMV structure as well as its denatured coat proteins. Lastly, the display of CBP-biotin on CPMV was validated by TEM and immunogold staining by using streptavidin probes conjugated with 5 nm sized gold nanoparticles. The micrographs revealed the immunogold staining only on CPMV-CBP-biotin (pointed by red arrows in Figure 3D) and nonspecific binding to native

CPMV was not observed. Also, the micrographs demonstrate the CPMV maintained their structural integrity after attachment of CBP-biotin.

Next, we performed a series of enzyme-linked immunosorbent assays (ELISAs) using the CBP-FITC and CBP-biotin to further probe their binding affinity to CPMV. CBP-biotin was coated onto a streptavidin-functionalized plate; this was followed by incubation with CPMV (CPMV was omitted for the control) (Figure 4A). Both sample (with CPMV) and control (without CPMV) were then probed with a rabbit anti-CPMV polyclonal antibody followed by a goat anti-rabbit secondary antibody conjugated with HRP. Data are consistent with CPMV binding to CBP-biotin (unpaired t test, $p < 0.0001$ vs control) (Figure 4A). Next, a titration ELISA was performed by using constant amount of CBP-FITC to probe against a serial dilution of CPMV (0–10 μg of CPMV). Fluorescent intensity of bound CPMV-CBP-FITC was recorded and showed a typical dose–response curve with saturation reached over the concentrations tested (Figure 4B).

To determine the dissociation constant K_D, competition binding ELISAs were performed. Here binding of synthetic CBPs (used in a dilution series) to CPMV was competed against MP_{SEF} phage (used as constant amount). MP_{SEF} was detected by using HRP-conjugated anti-M13 monoclonal antibodies and measurement at $OD_{450\ nm}$. CPMV-bound MP_{SEF} ($OD_{450\ nm}$) is inversely proportionate to the amount of peptide added for competition. The amount of MP_{SEF} binding to CPMV reduced with the increasing amount of synthetic peptides added subsequently yielded lower absorbance value (Figure 4C,D). The half maximal inhibition concentration (IC_{50}) of both CBP-biotin and CBP-FITC tabulated was 0.17 μg (1.14 μM) and 0.56 μg (3.34 μM), respectively. CBP-biotin demonstrated a significantly lower dissociation constant K_D (~7 nM) compared to CBP-FITC (~0.7 μM). Different modes of peptide modification resulted different IC_{50} and K_D values despite having the exact same sequence. The FITC fluorophore modification may impair protein binding of the CBP ligand, as has been observed with other systems and can be explained by stereochemical hindrance.[28] The difference in charge of CBP-FITC vs CBP-biotin may also contribute to the differences in binding affinity.[29] CBP-FITC is negatively charged, and therefore electrostatic repulsion between CBP-FITC and CPMV may weaken the interaction; in contrast, biotin does not carry a charge. Hence, caution needs to be exercised when choosing the type of peptide modification to avoid the detrimental effect on the binding affinity.

HER2-Targeted CPMV by Use of Dual-Functional CBP-AHNP.

To demonstrate the applicability of the CBP to label and introduce an active ingredient to CPMV, we chose to label CPMV with a receptor targeting ligand. Specifically, we made use of the anti-HER2/neu-peptide (AHNP) peptide with demonstrated specificity for the human growth factor receptor 2 (HER2).[30] AHNP is a cyclic peptide (FCDGFYA-CYMDV; the peptide is cyclized via the Cys side chains, highlighted as C) derived from monoclonal antibody trastuzumab, and it has been shown that this minimal sequence binds to p185HER2/neu with high affinity (K_D = 300 nM).[31] HER2 is transmembrane protein tyrosine kinase receptor that has linked to human cancers.[32]

The dual functional CBP-AHNP peptide was synthesized inline with AHNP appended to the C-terminus of the CBP domain. A control peptide (*AHNP) without the CBP domain was also synthesized; both peptides were modified with a FITC label at their C-terminus (Figure 5A). CPMV-CBP-AHNP and controls were characterized by native agarose gel electrophoresis as described above. Colocalization of the fluorescent signal (from the FITC-labeled CBP-AHNP peptide) with the RNA and protein band from CPMV indicates successful labeling of CPMV with CBP-AHNP (Figure 5B, Lane 2). No fluorescent band was observed when *AHNP was incubated with CPMV (Figure 5B, Chemiluminescence panel, Lane 3), demonstrating there is no nonspecific interaction between *AHNP and CPMV.

Next, we assayed cell uptake of CPMV-CBP-AHNP vs CPMV using a HER2+ ovarian cancer cell line, SKOV3. We also assayed cell uptake using murine macrophages (RAW264.7 cells) to monitor nonspecific vs targeted uptake in immune cells vs cancer cells. For these experiments, CPMV samples were prepared by incubating CPMV with a 100 molar excess of AHNP peptides (CBP-AHNP or *AHNP) in 0.1 M KP buffer; excess peptides were removed by dual-step purification as described above. The FITC-label allows to track the peptides, and the CPMV carrier was detected be immunostaining using rabbit anti-CPMV polyclonal antibodies followed by staining with a Cy5-labeled goat anti-rabbit secondary antibody. The Cy5 label is spectrally distinct from FITC, and therefore the CPMV carrier and peptide ligand (FITC-labeled CBP-AHNP) can be detected simultaneously.

Macrophages were used to monitor nonspecific phagocytosis—both targeted and nontargeted CPMV nanoparticles are expected to be cleared by phagocytic innate immune cells.[33–35] Indeed, flow cytometry indicates that CPMV, CPMV*AHNP, and CPMV-CBP-AHNP were taken up by the RAW264.7 cells; differences in cell uptake were not apparent (Figure 6A, APC channel). Differences were noted when analyzing the FITC channel, monitoring uptake of the peptide into cells: CPMV-CBP-AHNP showed a significantly higher percentage of FITC positive cells, about 3-fold higher than CPMV-*AHNP ($p < 0.0001$) and ~23-fold higher than CPMV only ($p < 0.0001$) (Figure 6A, FITC channel). This indicates that the soluble AHNP peptide is taken up by cells, but the CPMV nanoparticle is more effectively taken up.

Next, we assayed targeted uptake using the HER2+ SKOV3 ovarian cancer cell line.[36] Cell binding assays show that CPMV-CBP-AHNP had significantly greater interactions with the HER2+ cancer cell line compared to the control samples, with an ~4.2-fold (based on APC channel) and ~10-fold (based on FITC channel) increase in percent positive cells compared to nontargeted CPMV controls (Figure 6B). The background cell binding of CPMV and CPMV*AHNP may be explained by nonspecific nanoparticle–cell interactions or the fact that CPMV interacts with mammalian cells via surface expressed vimentin.[37]

CONCLUSIONS

We report the isolation of CPMV-binding peptides (CBP) that bind CPMV with high selectivity and affinity; cross-reactivity against other plant viruses was not observed. Biopanning resulted in isolation of four lead candidates and characterization assays to

evaluate the peptide-to-CPMV binding concluded that the motif “GWRVSEF/L” is the CPMV-specific motif with phenylalanine (F) at the seventh position being stronger than leucine (L). CBP, GWRVSEF, tagged with biotin, FITC or HER2-specific targeting peptide ANHP were synthesized, and we demonstrated that the active ingredient could be displayed on CPMV using the CBP strategy. CBP binds to intact virions and was found bound to the S and L protein denatured and bound to nitrocellulose membranes. The CBP functionalization strategy offers a new avenue for CPMV nanoparticle functionalization and should offer a versatile tool to add active ingredient that otherwise may be difficult to conjugate or display. As a proof-of-concept, we demonstrated loading of a small affinity tag, a fluorophore, and targeting ligand; however, the concepts could be applied to display peptide epitopes for vaccination or therapeutics for drug delivery or immunotherapy.

Supplementary Material

Refer to Web version on PubMed Central for supplementary material.

ACKNOWLEDGMENTS

This work was funded in part by a Galvanizing Engineering in Medicine (GEM) Award and NIH Grant R01-CA224605. Dr. He Hu and Yifeng Ma are thanked for contributing TEM and SDS-PAGE images of control particles: PhMV virus-like particles, TMGMV, and PVX, respectively. We thank Dr. Hema Masarapu, Sri Venkateswara University, Tirupati, India, for providing the plasmids for VLP expression.

REFERENCES

(1). Lomonossoff GP Cowpea Mosaic Virus. In Encyclopedia of Virology; Elsevier Ltd.: 2008; pp 569–574.

(2). Sainsbury F; Cañizares, M. C.; Lomonossoff, G. P. Cowpea Mosaic Virus: The Plant Virus-Based Biotechnology Workhorse. Annu. Rev. Phytopathol. 2010, 48, 437–455. [PubMed: 20455698]

(3). Chant SR Viruses Of Cowpea, Vigna Unguiculata L. (WALP.). Ann. Appl. Biol. 1959, 47, 565–572.

(4). Nkanga CI; Steinmetz NF The Pharmacology of Plant Virus Nanoparticles. Virology 2021, 556, 39–61. [PubMed: 33545555]

(5). Chung YH; Cai H; Steinmetz NF Viral Nanoparticles for Drug Delivery, Imaging, Immunotherapy, and Theranostic Applications. Adv. Drug Delivery Rev. 2020, 156, 214–235.

(6). Lizotte PH; Wen AM; Sheen MR; Fields J; Rojanasopondist P; Steinmetz NF; Fiering S In Situ Vaccination with Cowpea Mosaic Virus Nanoparticles Suppresses Metastatic Cancer. Nat. Nanotechnol. 2016, 11, 295–303. [PubMed: 26689376]

(7). Wang C; Fiering SN; Steinmetz NF Cowpea Mosaic Virus Promotes Anti–Tumor Activity and Immune Memory in a Mouse Ovarian Tumor Model. Adv. Ther. 2019, 2, 1900003.

(8). Patel BK; Wang C; Lorens B; Levine AD; Steinmetz NF; Shukla S Cowpea Mosaic Virus (CPMV)-Based Cancer Testis Antigen NY-ESO-1 Vaccine Elicits an Antigen-Specific Cytotoxic T Cell Response. ACS Appl. Bio Mater. 2020, 3, 4179–4187.

(9). Beatty PH; Lewis JD Cowpea Mosaic Virus Nanoparticles for Cancer Imaging and Therapy. Adv. Drug Delivery Rev. 2019, 145, 130–144.

(10). Shukla S; Wang C; Beiss V; Cai H; Washington T; Murray AA; Gong X; Zhao Z; Masarapu H; Zlotnick A; Fiering S; Steinmetz NF The Unique Potency of Cowpea Mosaic Virus (CPMV): In Situ Cancer Vaccine. Biomater. Sci. 2020, 8, 5489–5503. [PubMed: 32914796]

(11). Usha R; Rohll JB; Spall VE; Shanks M; Maule AJ; Johnson JE; Lomonossoff GP Expression of an Animal Virus Antigenic Site on the Surface of a Plant Virus Particle. Virology 1993, 197, 366–374. [PubMed: 7692669]

(12). Madi M; Mioulet V; King DP; Lomonossoff GP; Montague NP Development of a Non-Infectious Encapsidated Positive Control RNA for Molecular Assays to Detect Foot-and-Mouth Disease Virus. J. Virol. Methods 2015, 220, 27–34. [PubMed: 25864934]

(13). Yildiz I; Lee KL; Chen K; Shukla S; Steinmetz NF Infusion of Imaging and Therapeutic Molecules into the Plant Virus-Based Carrier Cowpea Mosaic Virus: Cargo-Loading and Delivery. J. Controlled Release 2013, 172, 568–578.

(14). Zampieri R; Brozzetti A; Pericolini E; Bartoloni E; Gabrielli E; Roselletti E; Lomonosoff G; Meshcheriakova Y; Santi L; Imperatori F; Merlin M; Tinazzi E; Dotta F; Nigi L; Sebastiani G; Pezzotti M; Falorni A; Avesani L Prevention and Treatment of Autoimmune Diseases with Plant Virus Nanoparticles. Sci. Adv. 2020, 6, eaaz0295. [PubMed: 32494704]

(15). Pokorski JK; Steinmetz NF The Art of Engineering Viral Nanoparticles. Mol. Pharmaceutics 2011, 8, 29–43.

(16). Wang Q; Lin T; Tang L; Johnson JE; Finn MG Icosahedral Virus Particles as Addressable Nanoscale Building Blocks. Angew. Chem., Int. Ed. 2002, 41, 459–462.

(17). Wen AM; Shukla S; Saxena P; Aljabali AAA; Yildiz I; Dey S; Mealy JE; Yang AC; Evans DJ; Lomonossoff GP; Steinmetz NF Interior Engineering of a Viral Nanoparticle and Its Tumor Homing Properties. Biomacromolecules 2012, 13, 3990–4001. [PubMed: 23121655]

(18). Porta C; Spall VE; Findlay KC; Gergerich RC; Farrance CE; Lomonossoff GP Cowpea Mosaic Virus-Based Chimaeras: Effects of Inserted Peptides on the Phenotype, Host Range, and Transmissibility of the Modified Viruses. Virology 2003, 310, 50–63. [PubMed: 12788630]

(19). Lomonossoff GP Antigen Delivery Systems III: Use of Recombinant Plant Viruses. In Mucosal Immunology, Two-Volume Set; Elsevier Inc.: 2005; pp 1061–1072.

(20). Smith GP Filamentous Fusion Phage: Novel Expression Vectors That Display Cloned Antigens on the Virion Surface. Science 1985, 228, 1315–1317. [PubMed: 4001944]

(21). Wu CH; Liu IJ; Lu RM; Wu HC Advancement and Applications of Peptide Phage Display Technology in Biomedical Science. J. Biomed. Sci. 2016, 23, 1–14. [PubMed: 26753721]

(22). Wellink J Comovirus Isolation and RNA Extraction. Methods Mol. Biol. 1998, 81, 205–209. [PubMed: 9760508]

(23). Chan SK; Du P; Ignacio C; Mehta S; Newton IG; Steinmetz NF Biomimetic Virus-Like Particles as Severe Acute Respiratory Syndrome Coronavirus 2 Diagnostic Tools. ACS Nano 2021, 15, 1259–1272. [PubMed: 33237727]

(24). Ph.D.-7 Phage Display Peptide Library Kit|NEB https://www.neb.com/products/e8100-phd-7-phage-display-peptide-library-kit#Product Information (accessed 2021-02-15).

(25). Bakhshinejad B; Zade HM; Shekarabi HSZ; Neman S Phage Display Biopanning and Isolation of Target-Unrelated Peptides: In Search of Nonspecific Binders Hidden in a Combinatorial Library. Amino Acids 2016, 48, 2699–2716. [PubMed: 27650972]

(26). Hu Y-F; Gao X-C; Xu T-Q; Dun Z; Yu X-L Characterization of Seven New Polystyrene Plates Binding Peptides from a Phage-Displayed Random 12-Peptide Library. Comb. Chem. High Throughput Screening 2016, 19, 283–289.

(27). Qiang X; Sun K; Xing L; Xu Y; Wang H; Zhou Z; Zhang J; Zhang F; Caliskan B; Wang M; Qiu Z Discovery of a Polystyrene Binding Peptide Isolated from Phage Display Library and Its Application in Peptide Immobilization. Sci. Rep. 2017, 7, 1–11. [PubMed: 28127051]

(28). Sun YS; Landry JP; Fei YY; Zhu XD; Luo JT; Wang XB; Lam KS Effect of Fluorescently Labeling Protein Probes on Kinetics of Protein-Ligand Reactions. Langmuir 2008, 24, 13399–13405. [PubMed: 18991423]

(29). Yin L; Wang W; Wang S; Zhang F; Zhang S; Tao N How Does Fluorescent Labeling Affect the Binding Kinetics of Proteins with Intact Cells? Biosens. Bioelectron. 2015, 66, 412–416. [PubMed: 25486538]

(30). Guan SS; Wu CT; Chiu CY; Luo TY; Wu JY; Liao TZ; Liu SH Polyethylene Glycol-Conjugated HER2-Targeted Peptides as a Nuclear Imaging Probe for HER2-Overexpressed Gastric Cancer Detection in Vivo. J. Transl. Med. 2018, 16, 168. [PubMed: 29921305]

(31). Park BW; Zhang HT; Wu C; Berezov A; Zhang X; Dua R; Wang Q; Kao G; O'Rourke DM; Greene MI; Murali R Rationally Designed Anti-HER2/Neu Peptide Mimetic Disables

P185(HER2/Neu) Tyrosine Kinases in Vitro and in Vivo. Nat. Biotechnol. 2000, 18, 194–198. [PubMed: 10657127]

(32). Bermont L; Algros MP; Baron MH; Adessi GL Relevance of P185 HER-2/Neu Oncoprotein Quantification in Human Primary Breast Carcinoma. Breast Cancer Res. Treat. 2000, 63, 163–169. [PubMed: 11097092]

(33). Wen AM; Le N; Zhou X; Steinmetz NF; Popkin DL Tropism of CPMV to Professional Antigen Presenting Cells Enables a Platform to Eliminate Chronic Infections. ACS Biomater. Sci. Eng. 2015, 1, 1050–1054. [PubMed: 27280157]

(34). Plummer EM; Manchester M Endocytic Uptake Pathways Utilized by CPMV Nanoparticles. Mol. Pharmaceutics 2013, 10, 26–32.

(35). Gonzalez MJ; Plummer EM; Rae CS; Manchester M Interaction of Cowpea Mosaic Virus (CPMV) Nanoparticles with Antigen Presenting Cells In Vitro and In Vivo. PLoS One 2009, 4, e7981. [PubMed: 19956734]

(36). Zanini E; Louis LS; Antony J; Karali E; Okon IS; McKie AB; Vaughan S; El-Bahrawy M; Stebbing J; Recchi C; Gabra H The Tumor-Suppressor Protein OPCML Potentiates Anti–EGFR- and Anti–HER2-Targeted Therapy in HER2-Positive Ovarian and Breast Cancer. Mol. Cancer Ther. 2017, 16, 2246–2256. [PubMed: 28775148]

(37). Koudelka KJ; Destito G; Plummer EM; Trauger SA; Siuzdak G; Manchester M Endothelial Targeting of Cowpea Mosaic Virus (CPMV) via Surface Vimentin. PLoS Pathog. 2009, 5, e1000417. [PubMed: 19412526]

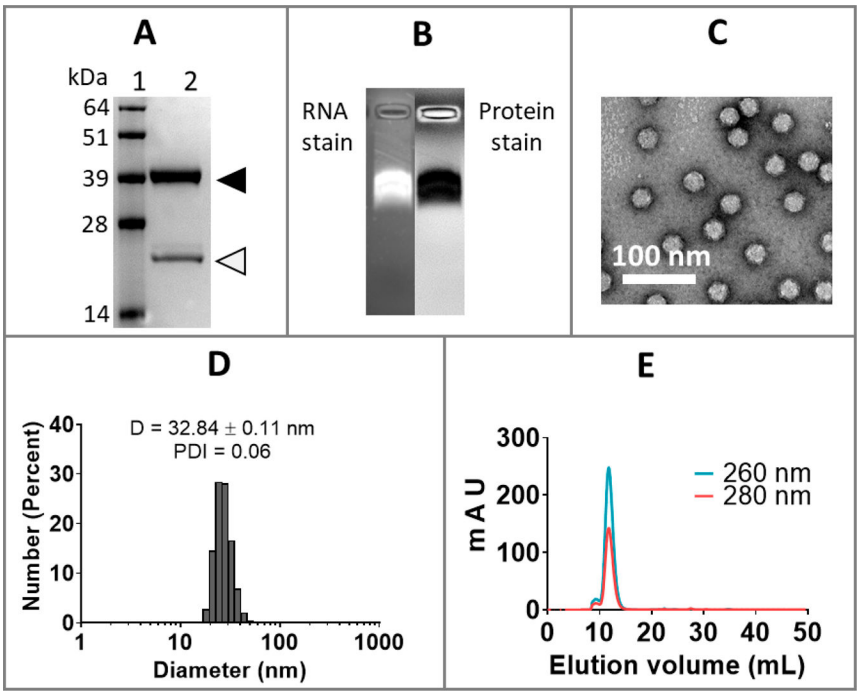

Figure 1.

Characterization of CPMV. (A) Denaturing sodium dodecyl sulfate polyacrylamide gel electrophoresis (SDS-PAGE). Lane 1 = SeeBlue Plus2 Prestained Protein Standard; Lane 2 = CPMV. Black triangle = large coat protein (42 kDa); open triangle = small coat protein (24 kDa). (B) Native agarose gel electrophoresis of CPMV where the same gel was stained with RNA stain GelRed (nucleic acid) and protein stain Coomassie Brilliant Blue (protein stain). (C) Negatively stained CPMV was analyzed by transmission electron microscopy (TEM). (D) Triplicate samples of CPMV were analyzed by dynamic light scattering (DLS), and the representative data sets are shown. *D* refers to average diameter of particles; PDI refers to polydispersity index. (E) CPMV analyzed by size exclusion chromatography (SEC) using a Superose 6 column. Nucleic acids were detected at 260 nm, and protein was detected at 280 nm.

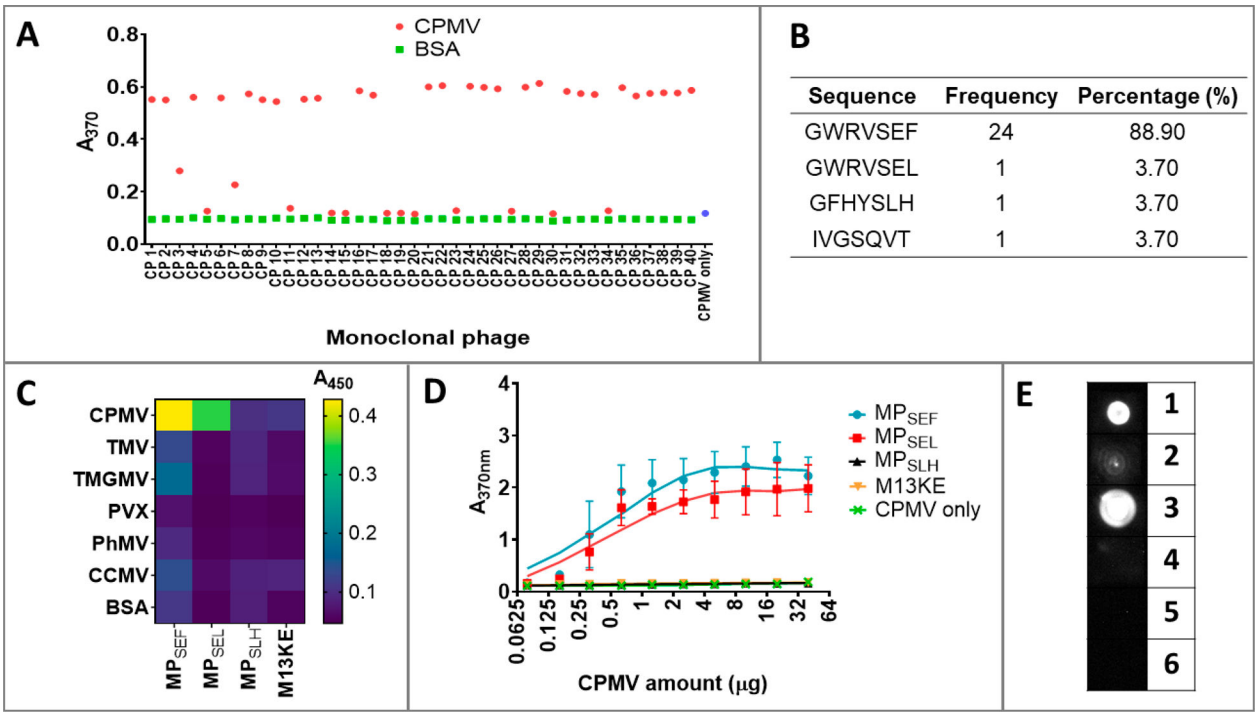

Figure 2.

Isolation and validation of CPMV binding monoclonal phages. (A) Monoclonal ELISA of monoclonal phages against CPMV (red dots) and BSA (green dots). CPMV only (blue dot) served as negative control to validate the binding of HRP-conjugated anti-M13 monoclonal antibody against CPMV. (B) Sequences of CPMV-binding peptides (CBPs) identified by DNA sequencing. (C) Heatmap showing cross-reactivity of monoclonal phages against CPMV vs other viruses. TMV: tobacco mosaic virus. TMGMV: tobacco mild green mosaic virus. PVX: potato virus X. PhMV: Physalis mottle virus (was used as VLP). CCMV: cowpea chlorotic mottle virus. BSA: bovine serum albumin (negative control). (D) Titration ELISA comparing binding of monoclonal phages across a serial concentration of CPMV. MP_{SEF}: GWRVSEF; MP_{SEL}: GWRVSEL; MP_{SLH}: GFHYSLH. Error bars show standard deviations for three replicates. (E) Dot blot to determine the specific binding of monoclonal phages (MP_{SEF}) to CPMV. (1) MP_{SEF} coated, probed with CPMV. (2) M13KE (empty phage) coated, probed with CPMV. (3) CPMV only (positive control). (4) BSA coated and probed with CPMV. (5) MP_{SEF} only (6) M13KE only. All samples were then incubated with primary antibodies (goat anti-CPMV rabbit polyclonal antibody) and subsequently with secondary antibodies (HRP conjugated goat anti-rabbit antibodies).

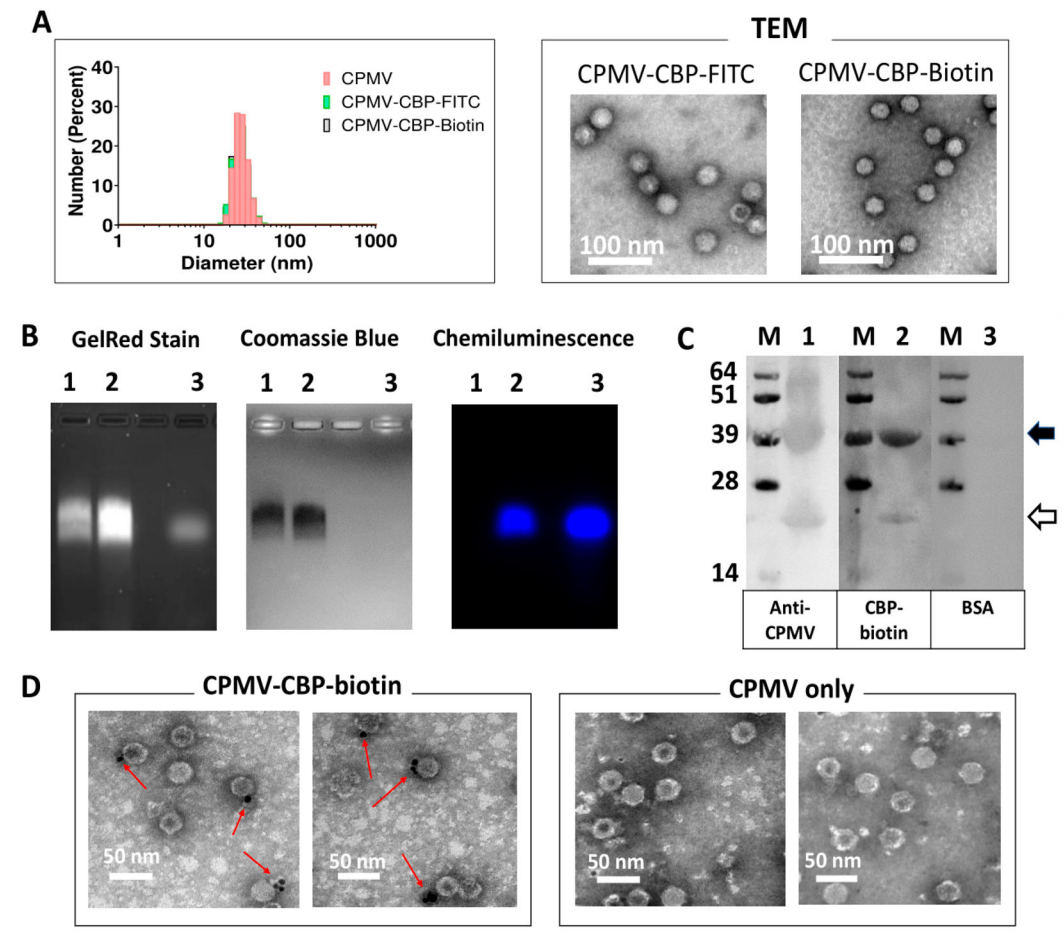

Figure 3.

Binding of CPMV-binding peptide (CBP) to CPMV. (A) Characterization of CPMV with noncovalent display peptides CBP-FITC and CBP-biotin. (B) Native agarose gel electrophoresis. (Lane 1) CPMV only. (Lane 2) CPMV with CBP-FITC. (Lane 3) CBP-FITC only. (C) Western blot analysis. CPMV on membrane was detected with (Lane 1) rabbit anti-CPMV polyclonal antibodies, followed by goat anti-rabbit monoclonal antibody conjugated with horseradish peroxidase (HRP); (Lane 2) CBP-biotin, followed by streptavidin HRP; (Lane 3) streptavidin HRP. Black arrow indicates CPMV large coat protein (~42 kDa), and open arrow indicates CPMV small coat protein (~24 kDa). M represents SeeBlue Plus2 Prestained Protein Standard. (D) Representative images from TEM with immunogold labeling. CPMV-CBP-biotin complex was stained with streptavidin-labeled with gold nanoparticles (5 nm); indicated by red arrows. Nonspecific binding of streptavidin-labeled gold nanoparticles to CPMV only was not observed.

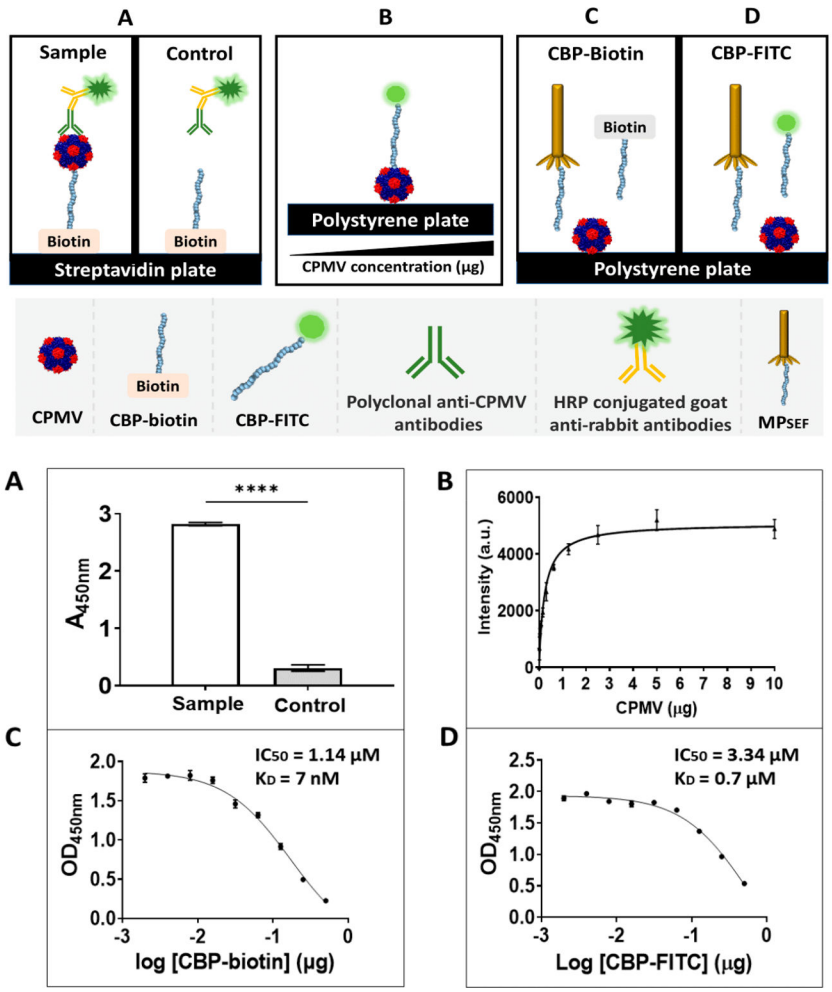

Figure 4.

Enzyme-linked immunosorbent assay (ELISA) of CBP binding to CPMV. Cartoon: (A) ELISA of CBP-biotin. (Sample) CBP-biotin coated onto streptavidin-functionalized plates followed by addition of CPMV; CPMV was omitted for the control group. This was followed by detection by using rabbit anti-CPMV polyclonal antibodies followed by HRP-conjugated goat anti-rabbit monoclonal antibodies. Results were compared by using unpaired *t* test (with ****$p < 0.0001$). (B) Titration ELISA of CBP-FITC against a range of CPMV concentrations. (C) Competitive ELISA between CBP-biotin (peptide) and MP_{SEF} (phage). (D) Competitive ELISA between CBP-FITC (peptide) and MP_{SEF} (phage). The half of maximal inhibitory concentration (IC_{50}) value was determined by GraphPad Prism by using nonlinear regression analysis (One site-Fit log IC50). All error bars show standard deviations for three replicates.

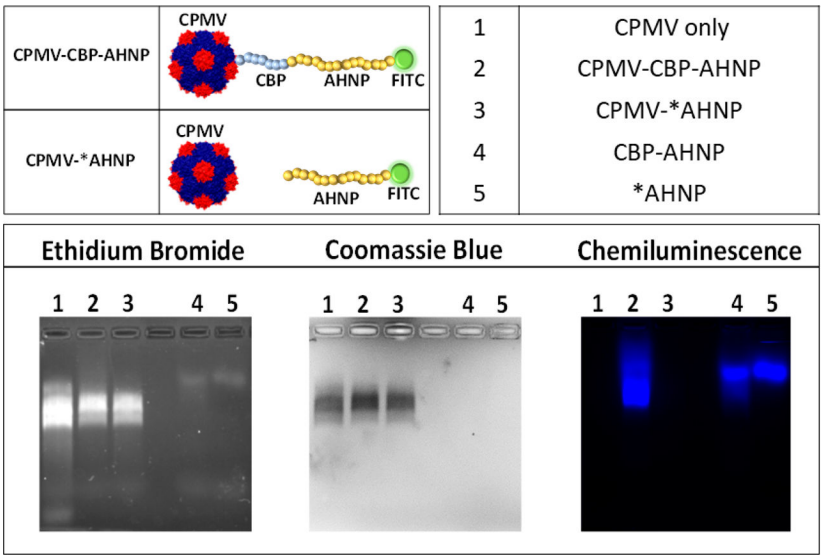

Figure 5.

Validation of CBP-AHNP binding to CPMV. Top panel: cartoon of peptides used; illustration of CPMV with CBP-AHNP and *AHNP. *AHNP without CBP domain acts as control and should not bind to CPMV; and bottom panel: Native agarose gel electrophoresis. (Lane 1) CPMV only. (Lane 2) CPMV-CBP-AHNP. (3) CPMV-*AHNP. (4) CBP-AHNP only. (5) *AHNP only.

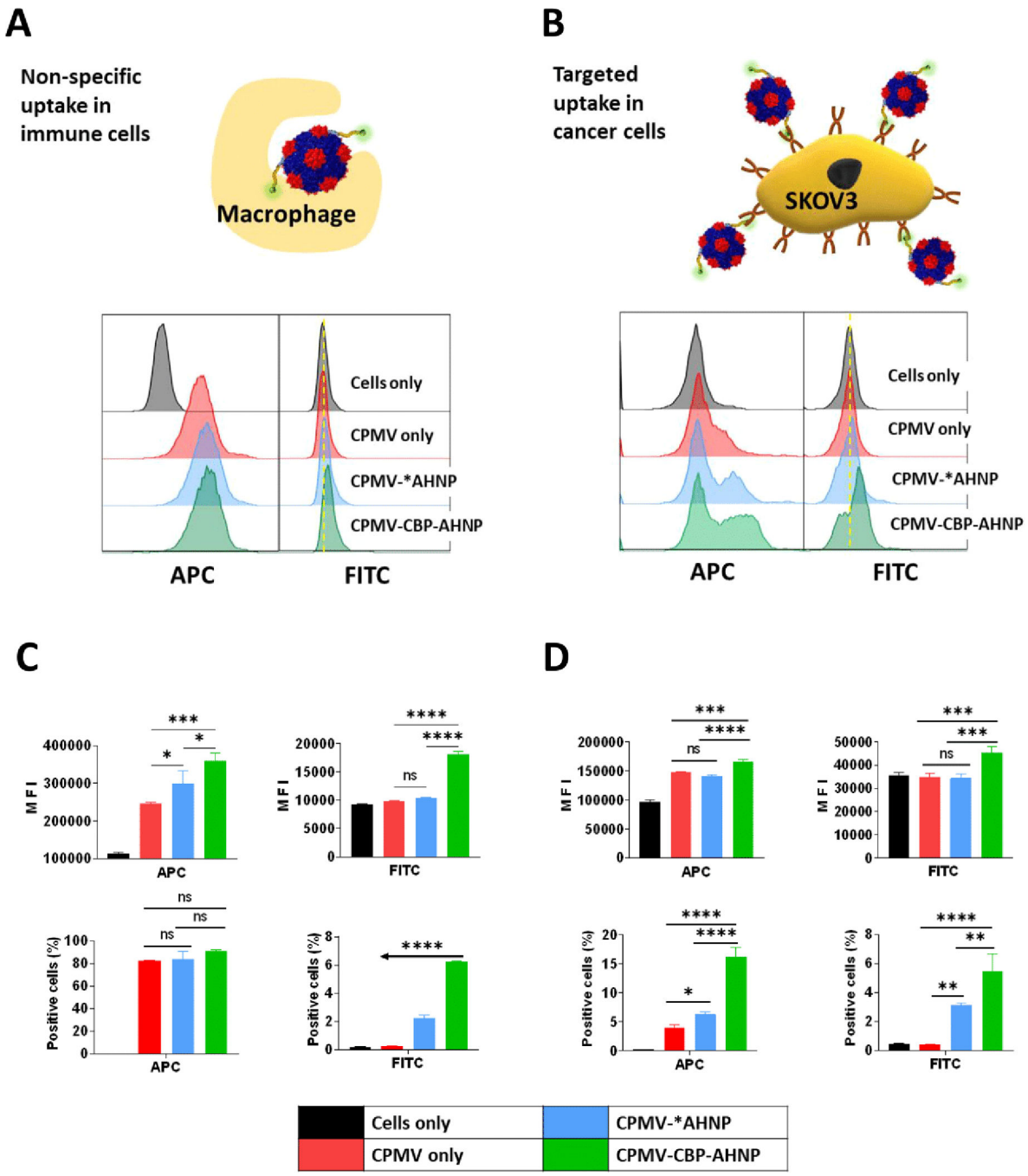

Figure 6.

CPMV-CBP-AHNP cell binding assays. Flow cytometry analysis was performed to assess cell uptake of CPMV, CPMV-*AHNP, and CPMV-CBP-AHNP particles by murine macrophages, RAW264.7 cells (A); as well as cell binding of the nanoparticle formulations to ovarian cancer cells, SKOV3 (B). Histograms and bar charts showing median fluorescent intensity (MFI) and % positive cells for the APC channel (Cy5 signal from CPMV staining) and FITC channel (FITC signal from labeled peptides) of RAW264.7 cells (C); and SKOV3

(D). Error bars indicate standard deviation. Statistical analysis was determined by one-way ANOVA with Tukey's test: ns $p > 0.05$, *$p \leq 0.05$, **$p \leq 0.01$, ***$p \leq 0.001$, ***$p \leq 0.0001$.